• Soil Rock

Methanogenesis from acetate Acetate formation from acetyl-CoA I Pyruvate fermentation to acetate II Pyruvate fermentation to acetate IV Pyruvate fermentation to ethanol III Pyruvate fermentation to acetate III L-glutamate degradation VII (to butanoate) Pyruvate fermentation to acetate I Pyruvate fermentation to acetate VII Malonate degradation I (biotin-independent) 1,4-Dihydroxy-2-naphthoate biosynthesis Mycolyl-arabinogalactan-peptidoglycan complex biosynthesis Superpathway of UDP-glucose-derived O-antigen building blocks biosynthesis Luteolin triglucuronide degradation Leukotriene biosynthesis Mycothiol biosynthesis Salicylate biosynthesis I Peptidoglycan biosynthesis II (staphylococci) Peptidoglycan biosynthesis IV (Enterococcus faecium) Peptidoglycan maturation (meso-diaminopimelate containing)

Row standard score:



b. Vellozia epidendroides Barbacenia macrantha



Hydrogen oxidation II (aerobic, NAD) Hydrogen production II Pyruvate fermentation to acetate III

		E
		L
		F
		F
		F
		S
		Ν
		A
		F
		(
		F
		(
		Ν
		S
		N
		·
		, (

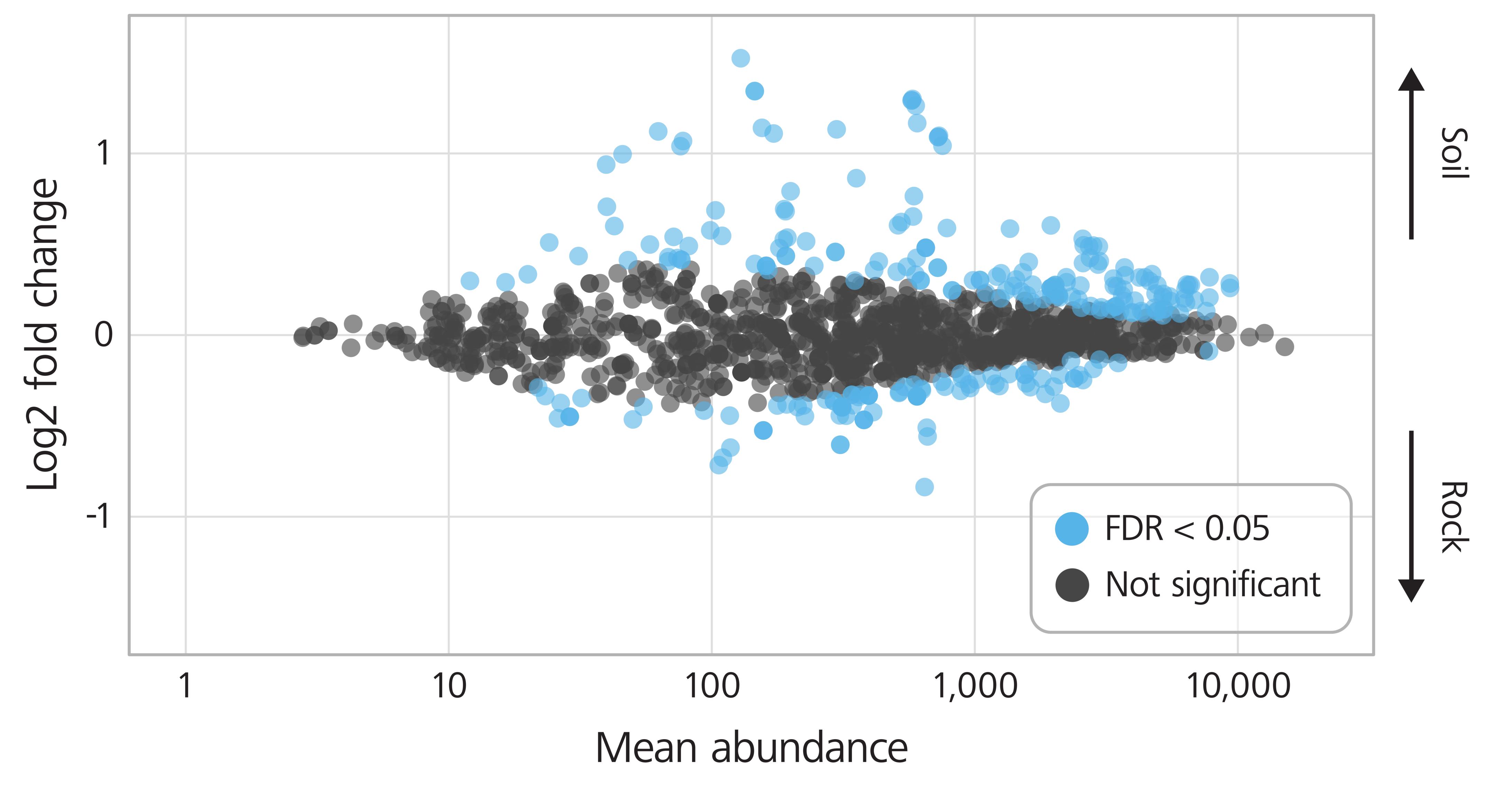
Estradiol biosynthesis I (via estrone) L-glutamate degradation VII (to butanoate) Pyruvate fermentation to acetate I Pyruvate fermentation to acetate VII Reductive monocarboxylic acid cycle Sulfoacetaldehyde degradation I Methanogenesis from acetate Arsenate detoxification III (mycothiol) Rutin degradation (plants) Cellulose and hemicellulose degradation (cellulolosome) Formaldehyde oxidation II (glutathione-dependent) Chlorophyllide a biosynthesis III (aerobic, light independent) Methylsalicylate degradation Salicylate degradation I Melibiose degradation Aclacinomycin biosynthesis Chlorophyllide a biosynthesis II (anaerobic)

Row standard score:

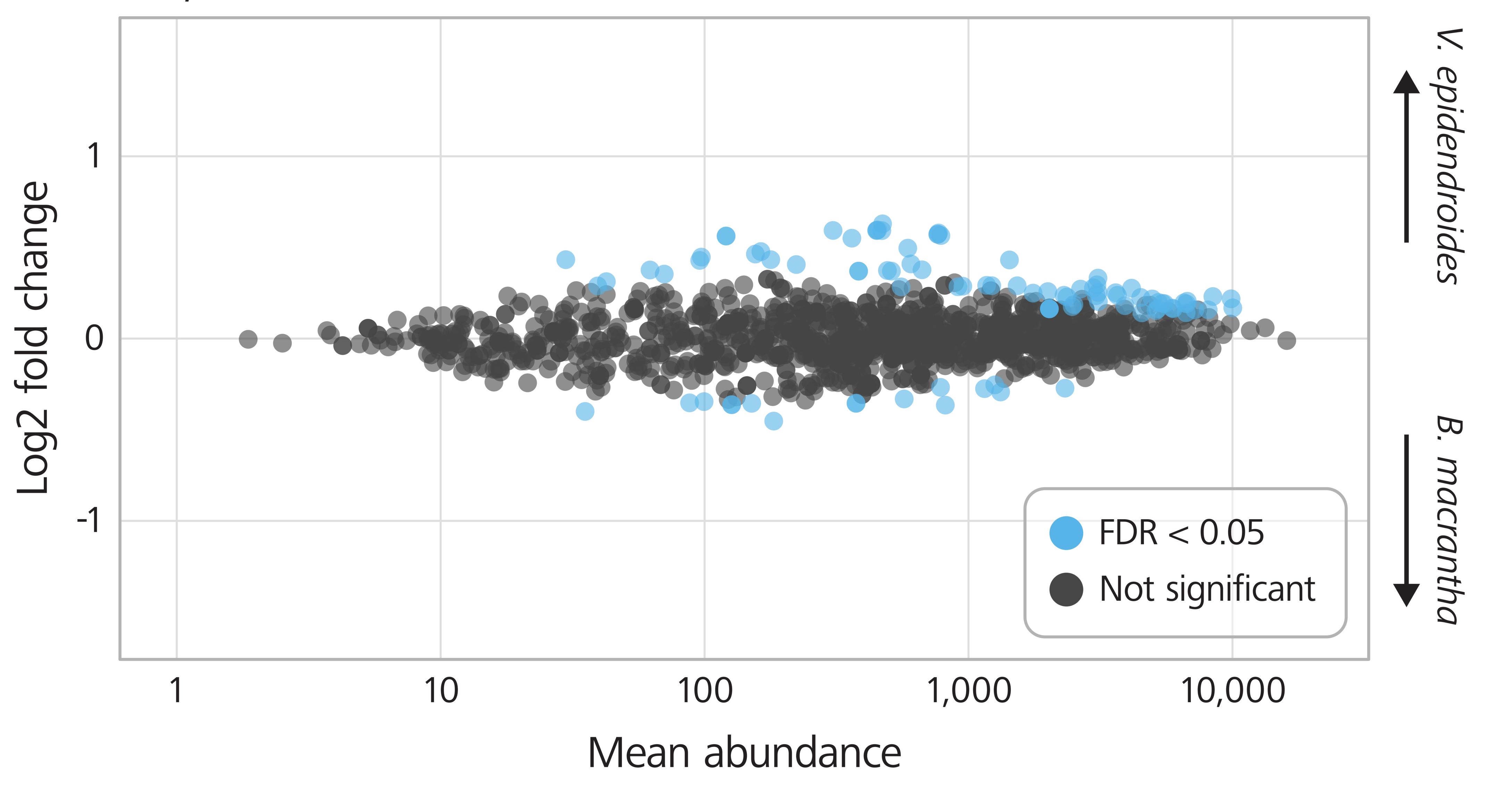
-1.5 -1 -0.5 0 0.5 1 1.5

Supplementary Figure S1. The metagenomes of microbial communities found in soil and rock exhibit major metabolic differences. Wald tests were performed to find differentially abundant MetaCyc pathways (a) between the soil and rock metagenomes and (b) between the *V. epidendroides* and *B. macrantha* root metagenomes. For each comparison, effect sizes (log2 fold change) were used for ordering and ten pathways from each end of the rank were selected for represention in heatmaps (a, b). For visualization, count values were transformed using the rlog function and standardized.

a. Soil vs. rock



D. *V. epidendroides* root vs. *B. macrantha* root



Supplementary Figure S2. Several metabolic pathways are differentially abundant between the studied environments. MA plots showing that a significant fraction of the MetaCyc pathways are differentially abundant (a) between the soil and rock metagenomes and (b) between the *V. epidendroides* and *B. macrantha* root metagenomes. Log2 fold change values were shrunken using a normal prior distribution centered on zero. FDR (false discovery rate) values were obtained by applying the Benjamini-Hochberg procedure to the p-values provided by the Wald test.